50th AIAA Aerospace Sciences Meeting including the New Horizons Forum and Aerospace Exposition
09 - 12 January 2012, Nashville, Tennessee
AIAA 2012-0409

Force Sensing of an Asymmetric Dielectric Barrier Discharge Using Mechanical Resonators

Mark D. Emanuel,[1] Douglas A. Bristow,[2] and Joshua L. Rovey[3]
Missouri University of Science and Technology, Rolla, MO, 65409

Current research into force sensing of a single dielectric barrier discharge (DBD) plasma actuator using mechanical resonators is examined. DBD plasma actuators, using alternating current, generate pulses of plasma at frequencies in the kHz range. The body force from the plasma changes with each pulse cycle, and can be measured and profiled using remote sensing from sensitive laser interferometry. Instead of simply measuring displacement of the actuator, different harmonics of the base frequency are measured to a high degree of precision using mechanical resonators. The frequency-dependent displacement data obtained from the resonator measurements are used to compute time-varying force generated by the plasma discharge. An example resonator is demonstrated to amplify motion more than 100X, and three harmonics with representative resonators are shown to accurately reconstruct the force profile of a DBD actuator.

Nomenclature

ω	=	Resonant frequency (rad/s)
E	=	Young's modulus (Pa)
l	=	Length (m)
g	=	Force due to gravity (m/s^2)
θ	=	Angle (rads or degrees)
x	=	Position (m)
X	=	Fourier series displacement (m or nm)
y	=	Position (m)
Y	=	Fourier series displacement (m or nm)
f	=	Force (N or mN)
F	=	Fourier series force (N or mN)
T_0	=	Fundamental period (s)
θ_k	=	Fourier series phase
c_k	=	Fourier series coefficient
ω_0	=	Fundamental frequency (rad/s)
k	=	Integer of harmonic
t	=	Time (s)
C	=	Beam constant
R	=	Resolution of system (m or nm)
Q	=	Q-Factor

[1] Graduate Research Assistant, Department of Mechanical and Aerospace Engineering, 400 W. 13th Street, Student AIAA Member.
[2] Assistant Professor of Mechanical Engineering, Department of Mechanical and Aerospace Engineering, 400 W. 13th Street.
[3] Assistant Professor of Aerospace Engineering, Department of Mechanical and Aerospace Engineering, 400 W. 13th Street, Senior AIAA Member.

I. Introduction

PLASMA generated by a single dielectric barrier discharge (DBD) has been under intensive research for several years. One well-documented use of DBD plasmas is flow control actuation.[1-4] Plasma actuators of the DBD variety are simplistic in their nature. A graphic portraying the physical configuration of a DBD is given in Figure 1. The mechanism of action is straightforward. A grounded buried conductor is separated from an exposed high voltage conductor by a small dielectric layer. A potential difference applied between electrodes is sufficient to break down the air and form a layer of plasma at the edge of the exposed electrode. Somewhat unique to the general field of plasma study is that the actuator DBD can operate at atmospheric pressures. Ambient air molecules are charged and then accelerated away from the barrier creating a small body force on the actuator (or conversely the air) when excited by the plasma discharge.

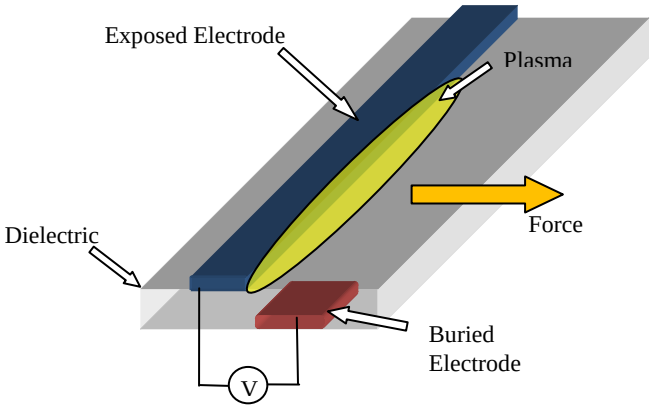

Figure 1. Physical Layout of A DBD Plasma Actuator

Plasma actuators are driven by high voltage, high frequency alternating current, creating a non-constant plasma force. In fact, previous work has shown that for every alternating current cycle, plasma is created twice: once during the forward stroke and once during the backward stroke.[5] Whereas studies of optimizing plasma (and, thus, force) generation are ongoing, there is a need to clarify how the plasma body force varies with respect to time. Other previous works have involved using optical and mechanical methods to identify the time-varying force.[6,7] Specifically, dual-mode time-resolved plasma forces involving a PUSH-push and push-pull force have been investigated. Original works by Baird et al[8] have utilized acoustic derivation to determine a PUSH-push force, and have recently been investigated by Font et al[9] using a resonant actuator. Optical derivation of a push-pull force has been measured by Porter et al.[10] The challenge here is that the inertia of the actuator body acts like a filter, eliminating the higher frequency harmonics of the plasma force. The approach presented in this paper is to amplify the high frequency harmonics by attaching a series of mechanical resonators to the actuator body. A combination of high plasma frequency in the kilohertz range, along with minute force on the order of millinewtons[10], results in plasma actuator vibrational displacement on the order of a few nanometers. Therefore, high frequency sampling and sub-nanometer displacement measurement is necessary to obtain a reasonably accurate view of how the plasma discharge imparts force on the actuator and air. Mechanical resonators allow for more detailed measurements of displacement, and when analyzed with Fourier analysis, allow for more detailed insight into time-varying DBD forces.

While measurements of the time-varying force profile have yet to be obtained, it is well known that the DC (average) force of DBD plasma actuators is on the order of tenths of a gram per foot of actuator.[11] To capture the time-varying force profile, a force sensor will need to have resolution of fractions of a gram and a bandwidth several times larger than the drive frequency of the DBD. There are no sensors available with that combination of resolution and bandwidth. The alternative approach developed by Font et al[9] is to mount the actuator so that the time-varying force accelerates the actuator to result in a time-varying position. The position can be measured remotely with sub-nanometer resolution and MHz bandwidth using laser interferometry. Based on features of the measured position signal, characteristics of time-varying force can be inferred.

The approach proposed here builds on the Font method with the goal of obtaining quantified, high resolution measurements of the time-varying force. Our method is to attach mechanical resonators to the actuator, with each resonator tuned to a harmonic of the time-varying force. The harmonics are determined by multiplying an integer times the base frequency. For example, if the original plasma generating frequency is at 3 kHz, then higher order harmonics include 6 kHz, 9 kHz, etc. The amplified motion of each resonator is measured by a laser interferometer. Using dynamic models of the apparatus, the time-varying force can be reconstructed from these measurements. The key benefit of this approach is the use of harmonic signals that can be averaged over many cycles to obtain very low noise. Combined with the mechanical amplification, the approach can yield very precise estimates of the time-varying force profile.

The rest of the paper is organized as follows. In Section 2 the physics of a freely hanging actuator and mechanical resonator is discussed, followed by the mathematical theory for force reconstruction from resonator

displacement measurements. Section 3 discusses the hardware and instrumentation setup used in the experiment. Section 4 contains details about calibration of a mechanical resonator.

II. Sensor Modeling and Force Reconstruction

Our approach consists of two essential dynamic systems:

1) The plasma actuator that is mounted to freely hang with thin gauge wire, and
2) Mechanical resonators tuned and calibrated to the harmonic frequencies of the DBD alternating current.

By constructing models of both dynamic systems, and then inverting those models, it will be possible to reconstruct the plasma force from the measured motion of the resonators. The dynamic models are developed in the following two subsections.

A. Dynamic Model of the Free-Hanging Actuator

The DBD plasma actuator is mounted to a rigid rectangular material, referred to here as the actuator body, as shown in Figure 2. The body is hung like a porch swing; that is, a support wire is attached to each corner of the body, with the pair of wires on each side forming a triangle orthogonal to the body. An illustration is shown in Figure 2. In this drawing, *m* is the lumped mass of the body, *l* is the distance of the body to the point of attachment, θ is the angle of rotation of the body, x is the horizontal displacement of the body, f is the thrust force provided by the DBD actuator and g is gravitational acceleration. The dynamics of the body are given by the pendulum equation,

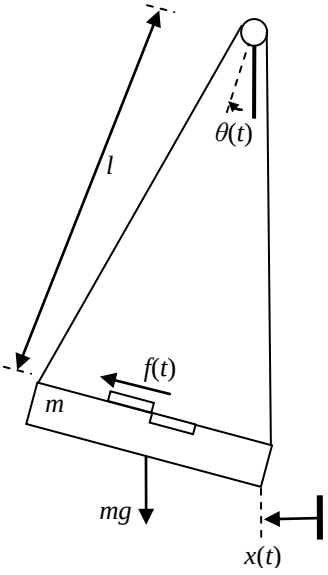

Figure 2. Schematic of the free hanging DBD actuator

$$ml^2\ddot{\theta} + mgl\sin\theta = lf \ . \tag{1}$$

Drag forces are neglected because velocities are very small. Linearizing (1) at the DC actuator force f_0, yields,

$$ml\ddot{\hat{\theta}} + kl\hat{\theta} = \hat{f} \tag{2}$$

where $\hat{\theta} = \theta - \theta_0$, $\theta_0 = \sin^{-1}\left(f_0/mg\right)$, $\hat{f} = f - f_0$, and $k = \left(mg/l\right)\sin\theta_0$. For small rotations, $x \approx l\theta$, so (2) can be written in linear coordinates as,

$$m\ddot{\hat{x}} + k\hat{x} = \hat{f} \tag{3}$$

where $\hat{x}$ is the differential linear motion measured from the DC offset. Taking the Fourier transform of (3) yields,

$$X\left(j\omega\right) = -\frac{1}{m\omega^2 - k}F\left(j\omega\right) \tag{4}$$

where X and F are the Fourier transform of $\hat{x}$ and $\hat{f}$, respectively. For analysis at high frequencies, (4) is approximated by,

$$X\left(j\omega\right) \approx -\frac{1}{m\omega^2}F\left(j\omega\right) \text{ for } \omega \gg \sqrt{k/m} = \sqrt{f_0/ml} \ . \tag{5}$$

Remark 1: Equation (5) provides the foundation for reconstructing DBD force from body position measurements. The motion X is inversely scaled by the body mass. Maximizing motion is desired to improve the fidelity of the measurements, and so, as is intuitive, a small mass should be used. Rigidity of the body material is also critical to ensure that the small forces are transformed into motion without losses; a rigid Styrofoam appears to be a good tradeoff of mass and rigidity. The length, *l*, of the wire supports are not critical as the frequencies, ω, of interest are in the range of thousands of rad/s, yielding a very good approximation in (5) independent of *l*.

The primary challenge in reconstructing the DBD force from the position measurements is the $1/\omega^2$ scaling that can result in very small motions for high frequencies, making accurate measurement difficult. Mechanical resonators attached to the actuator body can alleviate this challenge by greatly amplifying the motion. Modeling of the resonators is presented in the following section.

B. Dynamic Model of the Mechanical Resonators

There are a variety of architectures that can be used to create a mechanical resonator. One of the simplest is the double-clamped beam, illustrated in Figure 3. The resonant frequency for a double-clamped beam is well known[12] and given by,

$$\omega_{beam} = C\sqrt{\frac{E}{\rho}}\frac{t}{l_{beam}^2} \tag{6}$$

where ω_{beam} is the resonant frequency in rad/s, C=1.03 is a beam constant, E is Young's modulus for the material selected, ρ is the density of the material, t is the thickness of the beam, and l_{beam} is the length of the beam. A calibration procedure, discussed in Section 4, will be used to obtain the amplification factor, Q, and phase shift, ψ, of the resonator at its resonant frequency. These parameters allow us to find the relationship between the clamp motion, x, and amplified beam motion, y, as,

$$Y(j\omega_{beam}) = Qe^{j\psi}X(j\omega_{beam}). \tag{7}$$

Remark 2: To maximize the amplification factor, the beam thickness, t, should be kept small. The resonant frequency of the beam can be most easily adjusted by selecting the proper beam length.

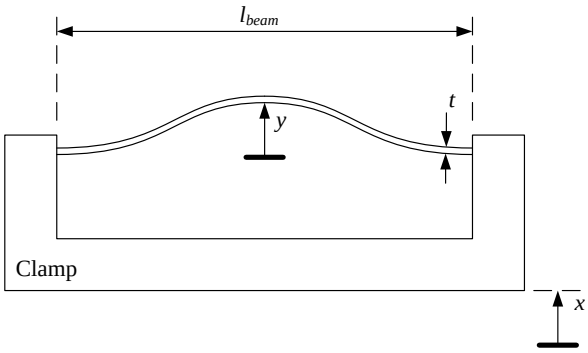

Figure 3. Schematic of a double-clamped beam

C. DBD Actuator and Mechanical Resonator Assembly

A schematic of the combined DBD actuator and mechanical resonator assembly is shown in Figure 4. The mechanical resonators are attached to the bottom of the actuator body to avoid interference of the induced air flow over the DBD actuator and the resonator. A laser interferometer is aligned to measure the center point of the resonator beam.

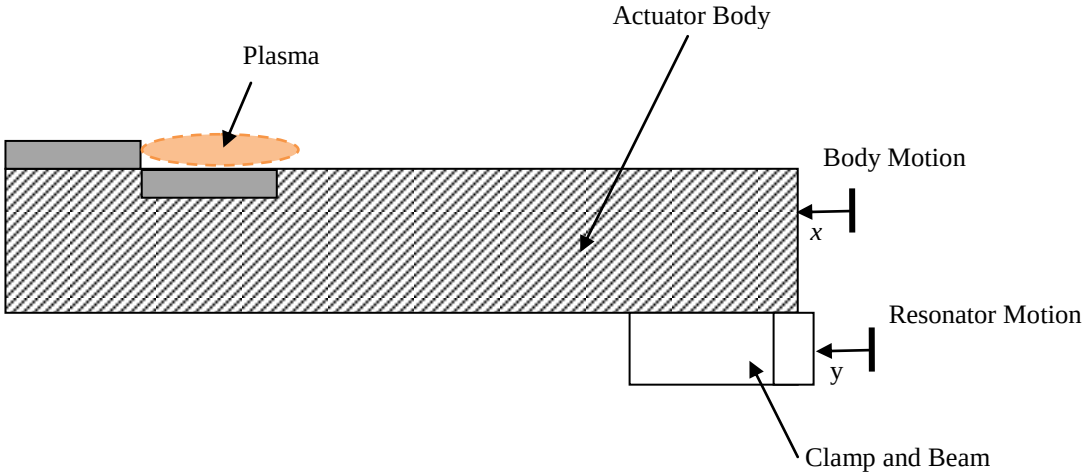

Figure 4. DBD Actuator and Resonator Assembly

D. Time-Varying Force Reconstruction

The time-varying force generated by the DBD actuator is periodic with a fundamental frequency equal to that of the DBD drive voltage frequency, ω_0. The time-varying force can therefore be written as a sum of harmonics,

$$\hat{f}(t) = \sum_{k=1}^{\infty} c_k \cos(k\omega_0 t + \phi_k), \tag{8}$$

or, in the frequency domain,

$$F(j\omega) = \sum_{k=1}^{\infty} c_k \delta(k\omega_0) e^{j\phi_k}, \tag{9}$$

where δ is the impulse function, $\delta(\omega) = 0$ for $\omega \neq 0$, $\int_{-\infty}^{\infty} \delta(\omega) d\omega = 1$. From (5) and (7), the motion of a resonator tuned to resonate at the k^{th} harmonic frequency is given by,

$$\begin{aligned} Y(jk\omega_0) &= -\frac{c_k Q_k}{mk^2\omega_0^2} e^{j(\psi_k + \phi_k)} \delta(k\omega_0) \\ &= \frac{c_k Q_k}{mk^2\omega_0^2} e^{j(\psi_k + \phi_k + \pi)} \delta(k\omega_0), \end{aligned} \tag{10}$$

and therefore, magnitude and phase measurements of the k^{th} harmonic resonator are given by,

$$Mag(k) = \frac{c_k Q_k}{mk^2\omega_0^2}, \tag{11}$$

and

$$Phase(k) = \psi_k + \phi_k + \pi. \tag{12}$$

The time-varying force coefficients can then be calculated as,

$$c_k = \frac{mk^2\omega_0^2 Mag(k)}{Q_k}, \tag{13}$$

and

$$\phi_k = Phase(k) - \psi_k - \pi. \tag{14}$$

In order to determine the accuracy of the reconstructed force, let R be the resolution with which the magnitude of the resonator motion can be measured. Then, the differential error in the k^{th} harmonic of the force is given by,

$$dc_k = \frac{mk^2\omega_0^2 R}{Q_k}. \tag{15}$$

Clearly, large resonator amplification gains (Q_k) will be necessary at high frequencies (ω_0) to accurately reconstruct the force.

E. Relevant Harmonic Range

An important practical question to answer is how many harmonics are needed to accurately recreate the force waveform. This is, of course, difficult to determine without a precise model of the time-varying force. However, previous works[6,7] have determined that PUSH-push profiles, containing one large push and one small push in each cycle, are common. A candidate PUSH-push force profile was construsted, and is illustrated in Figure 5. The fundamental frequency for this candidate is 3000 Hz. The Fourier magnitude and phase coefficients are shown in Figure 6 and Figure 7, which shows that the response is dominated by the first three harmonics. A reconstructed force profile containing only the first three harmonics is shown in Figure 8, which demonstrates good agreement with the original signal.

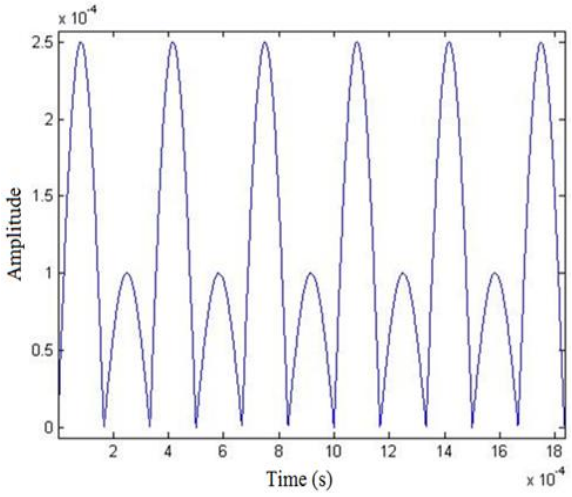

Figure 5. PUSH-push Candidate Force Function

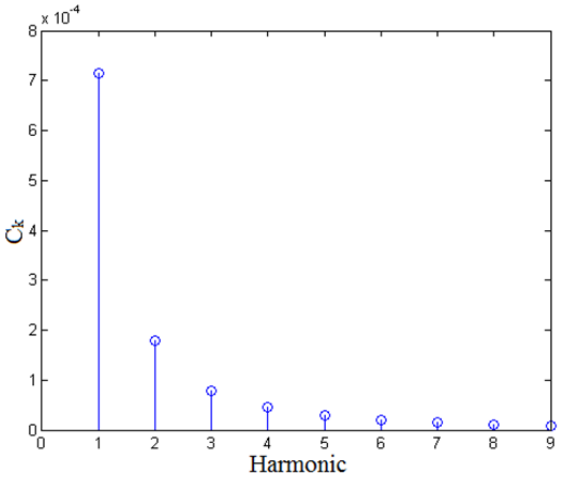

Figure 6. Fourier Series Coefficients Stem Plot for the First 9 Harmonics of a PUSH-Push Force Candidate

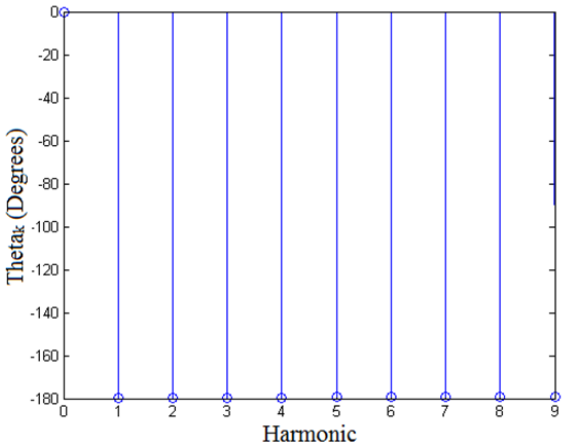

Figure 7. Fourier Series θ_k Stem Plot for the First 9 Harmonics of a PUSH-Push Force Candidate

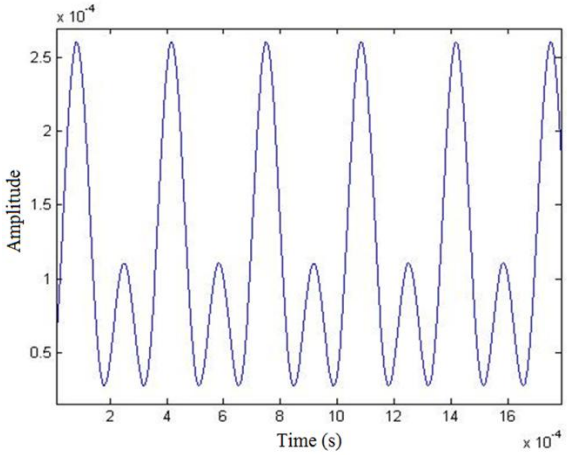

Figure 8. 3 Harmonic Fourier Series Reconstruction of PUSH-Push Force Candidate

III. Hardware Setup

A. Mechanical Resonator and Actuator

The beams for the mechanical resonator are fabricated from mirror finish stainless steel with a a thickness of 0.762mm. A mirror finish is critical to obtain accurate and consistent measurements of the beam displacement using a laser interferometer. A photograph of a clamp and beam assembly is shown in Figure 10. Final Resonator and Clamp Assembly with DBD Plasma Actuator in Background

The DBD actuator is constructed using Kapton tape, .06mm thick and 25.4mm wide. Conductors are 25.4mm wide adhesive-backed strips of copper tape, running a length of 292.1mm, with no overlap or gap between the

surface and buried electrodes. The mounting material is 5.5mm thick paper bounded Styrofoam, 304.8mm long and 76.2mm wide, for a total system mass of 20.81gm.

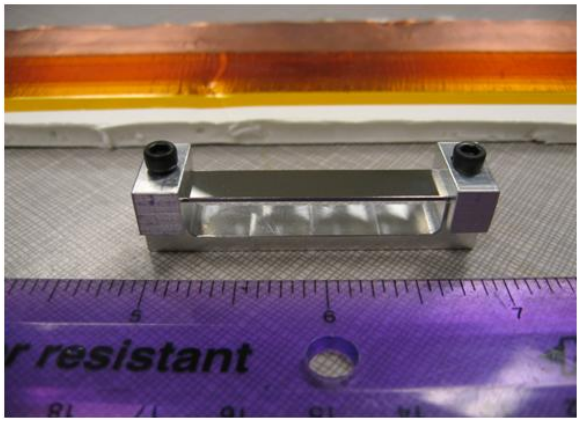

Figure 10. Final Resonator and Clamp Assembly with DBD Plasma Actuator in Background

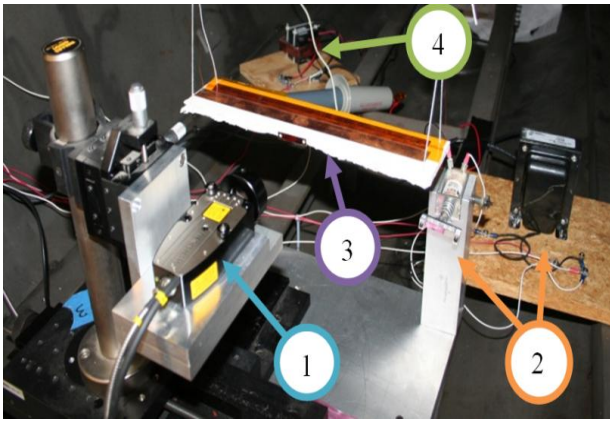

Figure 9. Physical Actuator and Resonator Calibration Testbed

Figure 10 shows the plasma actuator and resonator calibration testbed setup. The numbered items indicate:

1) Laser interferometer readhead
2) Solenoid and resonator calibration equipment
3) Freely hanging plasma actuator
4) High voltage transformer and probe equipment

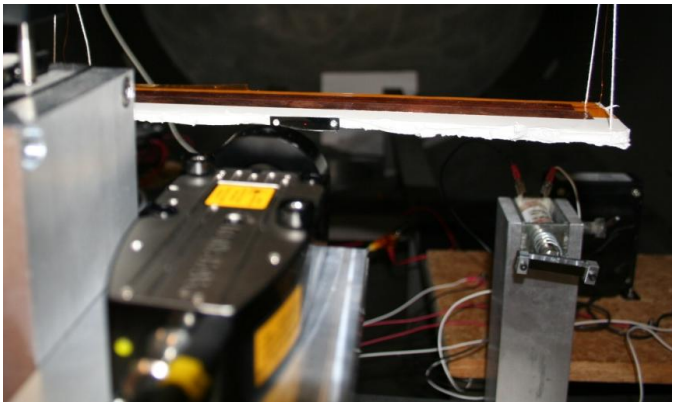

Figure 11. Closeup of Interferometer Readhead and Actuator

For testing and calibration purposes, the laser readhead is positioned directly in line with the center of the double clamped beam resonator, then repositioned to the clamp edge. Electronic components including a capacitor and high current inductor allow for the DC bias to "float" the solenoid piston, while permitting a signal generator to feed a driving voltage waveform to the solenoid coil. Plasma testing is conducted using the plasma actuator with the laser readhead positioned directly centered and in plane with the reflective resonator material, and uses a high voltage transformer tuned to resonate at 5kHz with an output capability between 1-10kHz at up to 10kV.

B. Sensors

Sensing of the resonator displacement is accomplished with a Renishaw model RLE10-SX-XD retroreflector laser interferometer, coupled with a Renishaw REE4000A50A quadrature interpolator. The minimum resolution output of the RLE10-SX-XD unit by itself is 20 nm. Based on a helium-neon laser with a wavelength of 633 nm, the REE4000A50A interpolates the interferometer output down to a final resolution of exactly 0.0791 nm.

The Renishaw interpolator unit has an output rate of 50MHz, requiring a digital oscilloscope capable of recording at 100MHz (the nyquist frequency). A Tektronix DPO2024 4-channel recording digital oscilloscope was procured, with a memory large enough to store 1.25 million data points, or 10ms of time at 125MHz.

Auxiliary sensors are used to record the applied voltage waveform of the plasma actuator, plus plasma current being generated. A Tektronix high voltage probe model P6015, with a 1000:1 input to output ratio, is used along

with a Pearson current monitor, model 4100, with a 1:1 volt to current ratio. Mating the two-channel quadrature output from the Renishaw interpolator into the digital oscilloscope allows for real-time data recording from all data sources.

In order for the interferometer to receive an adequate signal from the mechanical resonator, a reflectivity value of at least 50% is needed. Highly polished stainless steel is ideal for this application: the interferometer routinely detects 60% reflectivity or better. The digital quadrature output from the interpolator takes the form of a +/-5V square wave, requiring a post-processing program to decode the voltage into discreet steps. Displacement measurement is then derived from the status of the steps by comparing which channel (A or B) transitions before the other. MATLAB code is used extensively for this purpose, with an added benefit of precisely plotting voltage waveform input and plasma current on the same plot as displacement.

The interferometer laser read head is securely mounted to a 3-axis motion table to allow for in-plane, horizontal, and vertical positioning. In addition, the laser head mount has the capability to control pitch and yaw, so no matter what angle of attack the plasma actuator takes during actuation, the laser read head can be positioned to receive a reflection from the source.

IV. Resonator Calibration

Figure 13 shows the resonator and clamp calibration assembly. To provide a restoring force to the solenoid piston and clamp, a spring is mounted between the solenoid body and the clamp, then the spring is put under compression by applying the aforementioned DC offset. The entire assembly is placed horizontally and leveled.

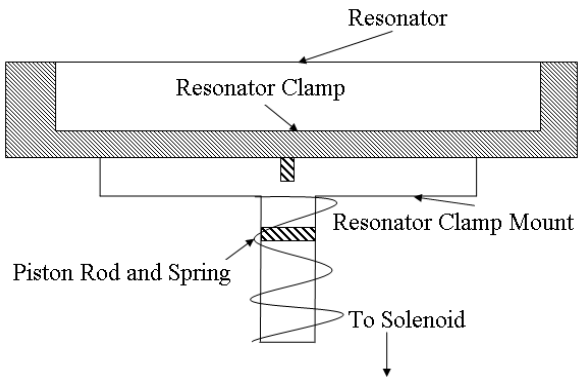

Figure 13. Solenoid Piston, Clamp, and Beam Assembly

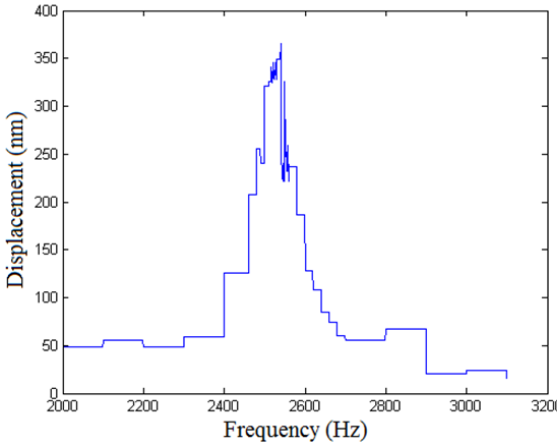

Figure 12. Calibration Plot for Mechanical Resonator: Beam Displacement

Figure 12 and Figure 14 shows the peak-to-peak displacement of the resonator and phase. A peak displacement and phase change occur at 2540Hz, indicating a resonant mode. Data for resonator displacement at the center of the beam was recorded along with base clamp displacement at a variety of frequencies near the resonant frequency. In each test, a sine wave signal at 10V peak-to-peak, with a constant DC offset of 360mA was applied to the calibration solenoid. MATLAB is used extensively for data post-processing, since displacement is only acquired from counting the pulses of quadrature output, and filtering out noise at unwanted frequencies is best performed by looking at FFT magnitudes of specific frequencies. Caution must be taken, though, when validating the results from the FFT calculation. Since an integer number of cycles are normally not recorded, the FFT computation will not precisely compute magnitude when calculating over a full recorded period. Consequently, only an integer number of beam cycles will be examined. Amplification here is computed based on dividing the beam motion by the base motion.

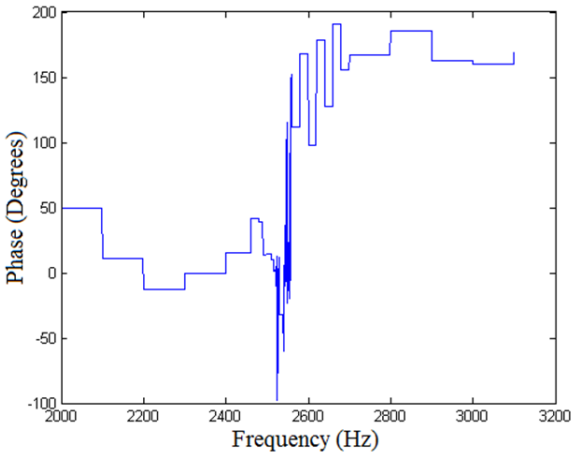

Figure 14. Calibration Plot for Mechanical Resonator: Beam Phase

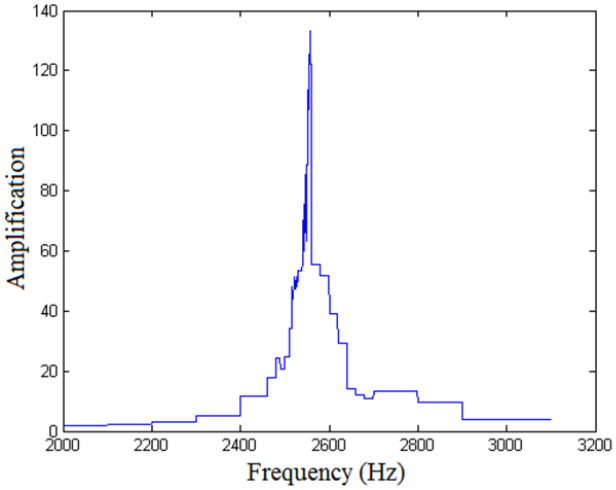

Figure 15. Amplification of Resonator vs Frequency

Figure 15 shows the amplification of the resonator at 10V, representing clamp motion of less than 1nm. The amplification factor is consistently in the 50X range, with a peak resonance above 100X. The real-world implication of this amplification is that if the plasma actuator is vibrating with a displacement of just a few nanometers, the mechanical resonator will be moving at least 50 times as much, yielding a larger displacement. Caution should be used when calculating amplification, as dividing large resonator displacements by small base clamp displacements that may cause the amplification to skew to higher values at higher frequencies. Thus, the frequency at which the beam phase changes from 0° to 180° in Figure 14, and not peak amplification, should be used to identify the resonance values.

V. Conclusion

In this experiment, mechanical resonators that resonate at desired frequencies are created to be mated to the underside of DBD plasma actuators. At least three harmonics, requiring three resonators, are needed to accurately replicate the force profile. A resonator is shown to amplify base motions successfully with a peak amplification above 100X at a specific frequency determined by a phase change. Using Fourier series analysis, plus high time-resolution and finely detailed displacement measurements, the force generated by the plasma generation cycle can be calculated. Potentially, the time-varying force calculation can identify not only the magnitude of the force created, but also the waveform of the force created, identifying whether the plasma body force is uni-directional or bi-directional.

Acknowledgments

The authors thank assistance from the Missouri University of Science & Technology Mechanical Engineering Tech Shop, including help from Joe Boze, Bob Hribar, and Randall Lewis. The authors also thank colleagues in the Precision Motion Control Laboratory and Aerospace Plasma Laboratory at Missouri University of Science & Technology for lengthy and fruitful discussions that added significantly to this project.

References

[1] Bolitho, M., and Jacob, J., "Use of Aggregate Plasma Synthetic Jet Actuators for Flow Control," AIAA Paper 2007-637, Jan. 2007.
[2] Thomas, F., Kozlov, A., and Corke, T., "Plasma Actuators for Bluff Body Flow Control," AIAA Paper 2006-2845, June 2006.
[3] Corke, T., Mertz, B., and Patel, M., "Plasma Flow Control Optimized Airfoil," AIAA Paper 2006-1208, Jan. 2006.

[4] Post, M., and Corke, T., "Overview of Plasma Flow Control: Concepts, Optimization, and Application," AIAA Paper 2005-0563, Jan. 2005.
[5] Corke, T. C., Post, M. L., Orlov, D. M., "Single Dielectric Barrier Discharge Plasma Enhanced Aerodynamics: Physics, Modeling, and Applications," *Review Article: Experiments in Fluids*, Center for Flow Physics and Control, University of Notre Dame
[6] Enloe, C. L., McHarg, M. G., and McLaughlin, T. E., "Time-Correlated Force Production Measurements of the Dielectric Barrier Discharge Plasma Aerodynamic Actuator," Journal of Applied Physics, Vol. 103, April 2008.
[7] Leonov, S., Opaits, D., Miles, R., Soloviev, V., "Time-resolved Measurements of Plasma-Induced Momentum in Air and Nitrogen Under Dielectric Barrier Discharge Actuation," *Physics of Plasmas*, No. 17, 2010.
[8] Baird, C., Enloe, C. L., McLaughlin, T. E., Baughn, J. W., "Acoustic Testing of the Dielectric Barrier Discharge (DBD) Plasma Actuator," AIAA Paper 2005–565, Jan. 2005.
[9] Font, G. I., Enloe, C. L., Newcomb, J. Y., Teague, A. L., Vasso, A. R., and McLaughlin, T. E., "Effects of Oxygen Content on the Behavior of the Dielectric Barrier Discharge Aerodynamic Plasma Actuator", AIAA Paper 2010-545, Jan. 2010.
[10] Porter, C. O., Baughn, J. W., McLaughlin, T. E., Enloe, C. L., Font, G. I., "Temporal Force Measurements on an Aerodynamic Plasma Actuator", AIAA Paper 2006-104, Jan. 2006.
[11] Ferry, J. W., and Rovey, J. L., "Thrust Measurement of Dielectric Barrier Discharge Plasma Actuators and Power Requirements for Aerodynamic Control," *5th Flow Control Conference*, 2010, Article number 2010-4982.
[12] http://lhotse.eng.yale.edu/wiki/uploads/3/3c/Standard_Equations.pdf